

Reversal of mouse hepatic failure using an implanted liver-assist device containing ES cell-derived hepatocytes

Alejandro Soto-Gutiérrez¹, Naoya Kobayashi¹, Jorge David Rivas-Carrillo¹, Nalu Navarro-Álvarez¹, Debaio Zhao², Teru Okitsu³, Hirofumi Noguchi³, Hesham Basma⁴, Yashuhiko Tabata⁵, Yong Chen¹, Kimiaki Tanaka¹, Michiki Narushima¹, Atsushi Miki¹, Tadayoshi Ueda⁶, Hee-Sook Jun^{7,8}, Ji-Won Yoon⁷, Jane Lebkowski⁹, Noriaki Tanaka¹ & Ira J Fox⁴

Severe acute liver failure, even when transient, must be treated by transplantation and lifelong immune suppression. Treatment could be improved by bioartificial liver (BAL) support, but this approach is hindered by a shortage of human hepatocytes. To generate an alternative source of cells for BAL support, we differentiated mouse embryonic stem (ES) cells into hepatocytes by coculture with a combination of human liver nonparenchymal cell lines and fibroblast growth factor-2, human activin A and hepatocyte growth factor. Functional hepatocytes were isolated using albumin promoter-based cell sorting. ES cell-derived hepatocytes expressed liver-specific genes, secreted albumin and metabolized ammonia, lidocaine and diazepam. Treatment of 90% hepatectomized mice with a subcutaneously implanted BAL seeded with ES cell-derived hepatocytes or primary hepatocytes improved liver function and prolonged survival, whereas treatment with a BAL seeded with control cells did not. After functioning in the BAL, ES cell-derived hepatocytes developed characteristics nearly identical to those of primary hepatocytes.

Acute liver failure can be a lethal condition requiring treatment by liver transplantation. It is frequently reversible, however, and many patients recover with conventional medical support. But because the natural history of acute failure varies widely, even transient hepatic failure, when severe, must be treated by transplantation and lifelong immune suppression¹. The shortage of donor livers, high cost and requirement for immunosuppression limit the use of this therapeutic modality. Treatment of hepatic failure can be improved by methods for temporary hepatic support. For example, in patients with fulminant liver failure, auxiliary liver transplants can be removed or allowed to undergo rejection when native liver function recovers. This form of therapy is also limited by the shortage of donor organs and by the risks associated with major surgery in the sickest patients^{1,2}. In addition, continuous hemodiafiltration with plasma exchange and albumin dialysis improve some parameters of hepatic function and are currently used as temporary support for many patients with acute liver failure^{3–5}, although improved survival has been difficult to document.

BAL^{6,7} devices contain active hepatocytes that remove toxins from the blood and supply physiologically active molecules important for recovery of hepatic function. Although BALs have successfully bridged

patients to organ transplantation, this technology has been limited by the lack of human livers as a source of hepatocytes. Potential alternative sources of hepatocytes include porcine hepatocytes^{8–10}, immortalized human hepatocytes¹¹, ES cell-derived hepatocytes^{12–15} and various adult stem cell sources such as oval cells, small hepatoblasts, hematopoietic stem cells and mesenchymal stem cells.

In this study, we show that 70% of cells derived from mouse ES cells were differentiated into hepatocyte-like cells by coculture with human liver cholangiocyte¹⁶, endothelial¹⁷ and stellate¹⁸ cell lines and growth in fibroblast growth factor (FGF)-2, human activin A and a deleted variant of hepatocyte growth factor (dHGF). ES cell-derived hepatocytes expressed liver-specific genes, secreted albumin and metabolized drugs nearly as well as primary mouse hepatocytes. We also describe a subcutaneously implanted BAL containing ES cell-derived hepatocytes that is easily recharged with additional cells, isolates the hepatocyte cell source from the recipient to reduce the risk of infection and teratoma formation, and does not require connection to the circulatory system, eliminating platelet consumption, hemodynamic instability and the increased risk of bleeding associated with the need for anticoagulants. Use of this device in

¹Department of Surgery, Okayama University Graduate School of Medicine and Dentistry, 2-5-1 Shikata-cho, Okayama 700-8558, Japan. ²Roslin Institute, Roslin, Midlothian EH10 4AN, UK. ³Department of Transplantation, Kyoto University Hospital, 54 Kawara-cho, Shogoin, Sakyo-ku, Kyoto, 606-8507, Japan. ⁴Department of Surgery, University of Nebraska Medical Center, Omaha, Nebraska 68198-3285, USA. ⁵Institute for Frontier Medical Sciences, Kyoto University, 54 Seigoin-Kawaracho, Sakyo-ku, Kyoto 606-8507, Japan. ⁶Division of Laboratory Products (T.U.), Dainippon Pharmaceutical Co., Ltd., Osaka. ⁷Rosalind Franklin Comprehensive Diabetes Center, Chicago Medical School, North Chicago, Illinois 60064, USA. ⁸Department of Biochemistry, Chosun University School of Medicine, 375 Seosuk-Dong, Gwangju 501-759, Korea. ⁹Geron Corporation, 230 Constitution Drive, Menlo Park, California 94025, USA. Correspondence should be addressed to I.J.F. (ijfox@unmc.edu) or N.K. (immortal@md.okayama-u.ac.jp).

Received 18 August; accepted 6 October; published online 5 November 2006; doi:10.1038/nbt1257

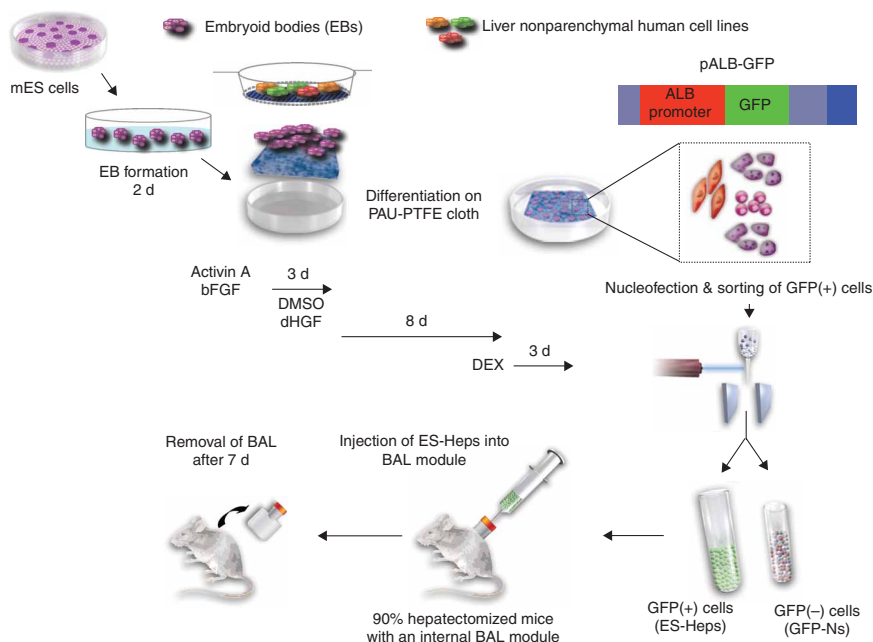


Figure 1 Schematic representation of the strategy for differentiation of mouse embryonic stem cells to hepatocytes and their use for BAL therapy. Mouse embryonic stem cells (mES cells) were cultured in suspension method for 2 d to form embryoid bodies (EBs). The resulting embryoid bodies were transferred onto unwoven polytetrafluoroethylene (PTFE) cloth and treated with fibroblast growth factor (FGF)-2 (100 ng/ml) and activin A (100 ng/ml) for 3 d, then cocultured with MMC-C-treated human nonparenchymal liver cell lines on Matrigel-layered trans-well membranes, with the deleted variant of hepatocyte growth factor (dHGF; 100 ng/ml) and 1% dimethyl sulfoxide (DMSO) for 8 d, and at the end stage with dexamethasone (DEX; 10^{-7} M) for 3 d. Finally, the cells were transduced with a plasmid containing green fluorescent protein (GFP) cDNA under the control of the albumin promoter (pALB-GFP). The GFP⁺ cells (ES-Heps) were used to inoculate a BAL module implanted into 90% hepatectomized mice. The GFP⁻ cells served as a negative control.

mice with acute liver failure, which uniformly die within 4 d of inducing hepatic failure, resulted in 90% long-term animal survival.

RESULTS

Differentiation of mouse ES cells into hepatocytes

To induce differentiation of mouse ES cells toward hepatocytes, we first generated embryoid bodies by growing the cells in suspension culture for 2 d. The embryoid bodies were transferred to a flask containing a poly-amino-urethane (PAU)-coated, nonwoven polytetrafluoroethylene (PTFE) fabric that allows cell adhesion, and cells

were cultured for 3 d in the presence of FGF-2 and human activin A. Cells were then cultured in the presence of mitomycin-C (MMC-C)-treated conditionally immortalized human liver nonparenchymal cells. Cells cocultured in this way were treated for 8 d in DMSO and dHGF and then cultured for 3 d in dexamethasone (Fig. 1).

Gene expression profile of mouse ES cell-derived hepatocytes

To determine the time course and degree to which ES cells were induced to differentiate into hepatocytes, we used reverse-transcriptase (RT)-PCR at various times during the culture process

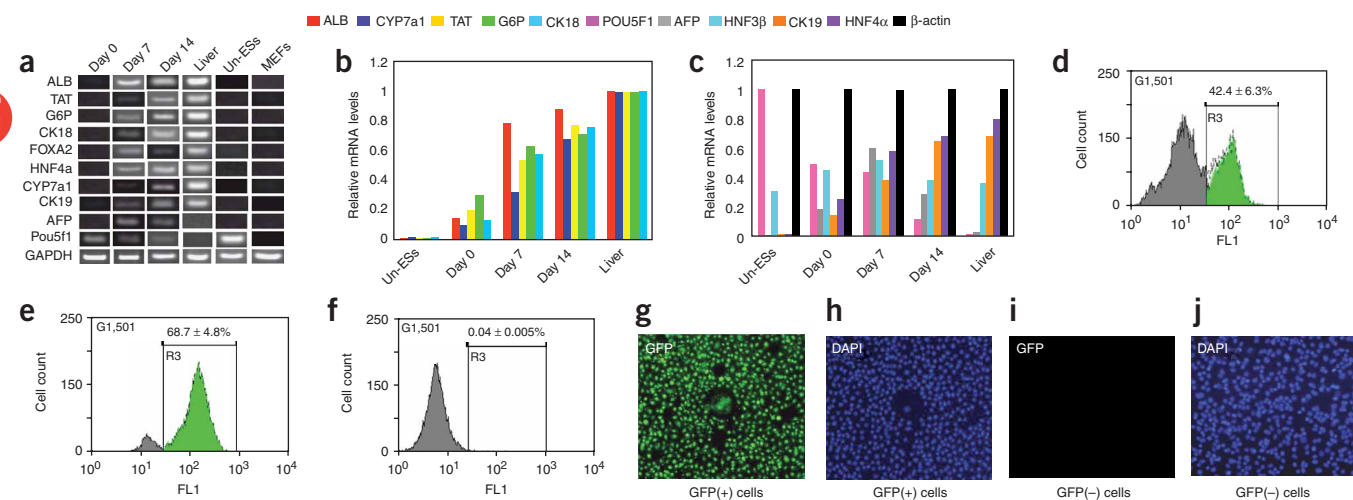


Figure 2 Characterization and purification of mouse ES cell-derived hepatocytes. (a) At 0, 7 and 14 d during the process of differentiating mES cells into hepatocytes, the expression of lineage-specific hepatic markers (ALB, TAT, G6P, CK18, CK19, and CYP7A1), endoderm markers (HNF-3 β , HNF-4 α and AFP) and a marker for undifferentiated cells (Pou5f1) were analyzed by RT-PCR. Mouse liver (Liver) served as the positive control, and undifferentiated mouse ES cells (Un-ESs) and mouse embryonic fibroblasts (MEFs) served as negative controls. (b,c) Expression profiles were confirmed by real-time RT-PCR analysis, and mRNA expression levels were normalized relative to beta-actin and normal adult mouse liver. (d-f) After 14 d of differentiation culture with growth factors alone (d) or with coculture using non-parenchymal cells (e), cells were transfected with pALB-GFP and analyzed by FACS. (f) Un-ESs transfected with pALB-GFP served as a control. (g,h) After MoFlo sorting, 100% of recovered cells were GFP-positive as confirmed by Dapi nuclear staining (h). (i,j) GFP-negative cells recovered by MoFlo served as control for BAL therapy. Scale bar, 100 μ m (g-j). The data are representative of at least three independent experiments. AFP, alpha fetoprotein; ALB, albumin; CK18, cytokeratin-18; cytokeratin-19; CYP7A1, cytochrome P450; G6P, glucose-6-phosphate; HNF-3 beta, hepatic nuclear factor-3 β ; HNF-4 α , hepatic nuclear factor-4 α ; TAT, tyrosine aminotransferase.

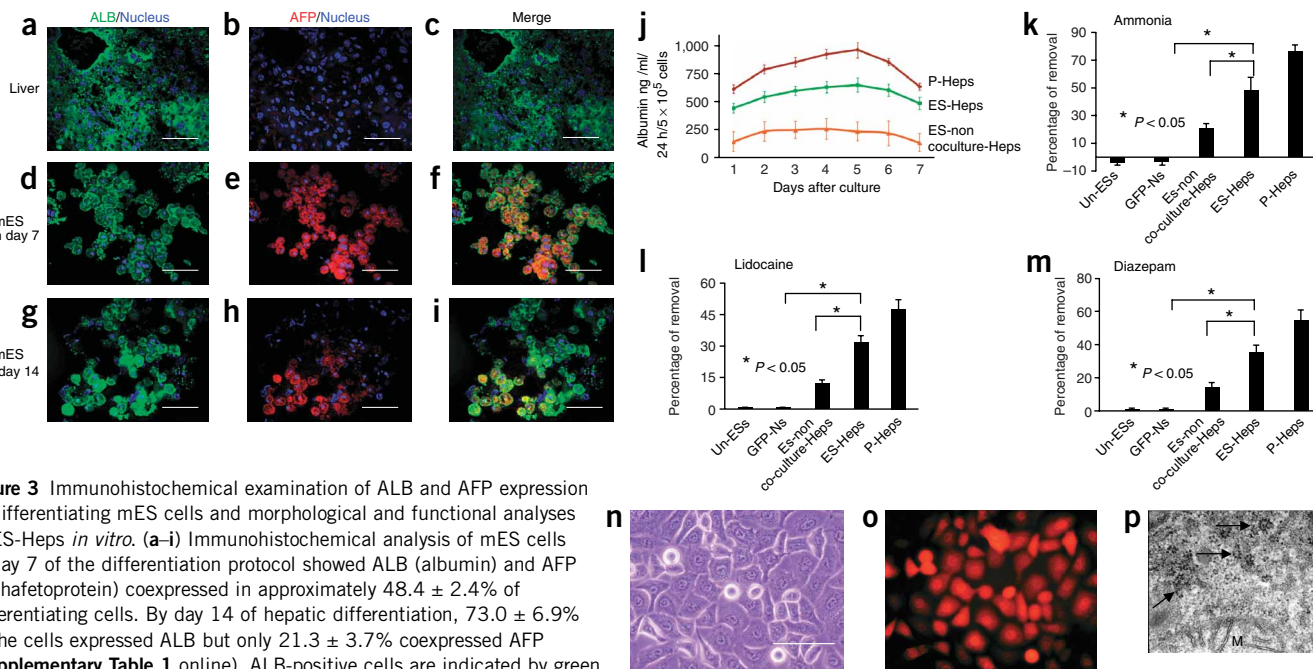


Figure 3 Immunohistochemical examination of ALB and AFP expression in differentiating mES cells and morphological and functional analyses of ES-Heps *in vitro*. (a–i) Immunohistochemical analysis of mES cells at day 7 of the differentiation protocol showed ALB (albumin) and AFP (alphafetoprotein) coexpressed in approximately 48.4 ± 2.4% of differentiating cells. By day 14 of hepatic differentiation, 73.0 ± 6.9% of the cells expressed ALB but only 21.3 ± 3.7% coexpressed AFP (Supplementary Table 1 online). ALB-positive cells are indicated by green fluorescence staining; AFP-positive cells are indicated by red fluorescence staining; nuclei are stained with DAPI blue. Mouse adult liver was used as control. Scale bar, 50 μm. (j) Albumin secretion by ES-Heps and mouse primary hepatocytes (P-Heps) was measured ($n = 5$). (k, l, m) We loaded ammonium sulfate (0.56 mM), lidocaine (100 mg/ml) (l) or diazepam (100 μg/ml) (m) into culture wells containing ES-Heps (5×10^5 cells). The amount remaining was measured 24 h later and the amount metabolized was calculated per mg cellular protein. (n, o) Light microscopy showed that ES-Heps were morphologically polygonal with enriched cytoplasmic granules (n) and immuno-positive for albumin (o). (p) Transmission electron microscopy showed accumulation of glycogen rosettes in ES-Heps (arrows). (n–p) Scale bar, 50 μm. (p) Original magnification $\times 30,000$. Undifferentiated mouse embryonic stem cells (Un-ESs) and GFP-negative cells (GFP-Ns) were negative controls, and P-Heps was a positive control ($n = 5$).

to analyze markers for endoderm-specific gene expression (alpha fetoprotein (*Afp*), hepatocyte nuclear factor (*Foxa1*)-3 β and *HNF-4 α*); hepatocyte-specific gene expression (albumin (*Alb1*), tyrosine-aminotransferase (*Tat*), glucose-6-phosphate (*G6pc*), cytokeratin 18 (*Krt18*), cytokeratin-19 (*Krt19*) and cytochrome P450 (*Cyp7a1*)); and for undifferentiated ES cells (*Pou5f1*). Hepatocyte-specific gene expression occurred within 7 d and increased by day 14 of differentiation, although the level of expression was somewhat lower than that of normal hepatocytes. Endoderm-specific gene expression was also increased. *Pou5f1* expression gradually decreased during culture with growth factors and feeder cells (Fig. 2a–c), confirming progressive differentiation toward hepatocytes in a population of cells, and *Afp* expression, which is present in endoderm but is not expressed by mature hepatocytes, was still detected 14 d after differentiation culture, indicating that differentiation toward a mature hepatocyte phenotype was not uniform.

Cells were further analyzed by RT-PCR to determine whether differentiation was liver specific (Supplementary Methods online). From day 0 to 7 of the differentiation program, mouse ES cells expressed genes specifically associated with definitive endoderm (*Gsc*, *Cdh3* and *Sax17*) and transiently expressed the primitive streak gene, brachyury, indicating induction of mesendoderm. Genes indicating differentiation toward ectoderm (*Ache* and *Pax6*) and mesoderm (*Nkx2.5* and *Gata-4*), a gene specific for pulmonary differentiation (*Spc*), pancreatic marker genes (*Ipf1* and *Neud4*) and a common hepatic-pancreatic transcription factor (*Onecut1*, formerly known as *HNF-6*) were also analyzed. None of the ectoderm, pulmonary or pancreatic marker genes was expressed in differentiating mES cells after day 7, but *Gata-4* and *Onecut1* expression was induced and

maintained until the end of the differentiation program (day 14), indicating development of endoderm-derived cells including common hepatic-pancreatic precursors (Supplementary Fig. 1 online).

Immunohistochemical staining of ES cell-derived hepatocytes (ES-Heps) showed that 48.4 ± 2.4% of mouse ES cells coexpressed albumin (ALB) and AFP on day 7 of the differentiation protocol. By day 14, 73.0 ± 6.9% of ES cell-derived cells expressed ALB, but only 21.3 ± 3.7% coexpressed AFP (Supplementary Table 1 online).

Coculture enhances differentiation of ES cells

To select ES cells that differentiated toward hepatocytes, we transfected embryoid body-derived cells with a plasmid vector containing the gene encoding green fluorescent protein (GFP) under the control of the albumin promoter (pALB-GFP). After transfection, embryoid body-derived cells expressing albumin would also express GFP. GFP expression was strongly affected by culture conditions. When embryoid body cells were cultured with growth factors only (without cell coculture), 42.4 ± 6.3% of cells actively expressed GFP and thus transcribed albumin. When embryoid body cells were cultured on conditionally immortalized human stellate cells, endothelial cells and cholangiocytes, the percentage of GFP-expressing cells increased to 68.7 ± 4.8% (Fig. 2d–f).

Characteristics of flow-sorted, albumin-expressing ES-Heps

Albumin-expressing, GFP-positive cells generated with and without cell coculture were isolated by a cell sorter MoFlo, and GFP expression was confirmed by fluorescence microscopy and Dapi nuclear staining (Fig. 2g, h). Incompletely differentiated, GFP-negative cells (GFP-Ns; Fig. 2i, j) were used as negative controls for subsequent experiments.

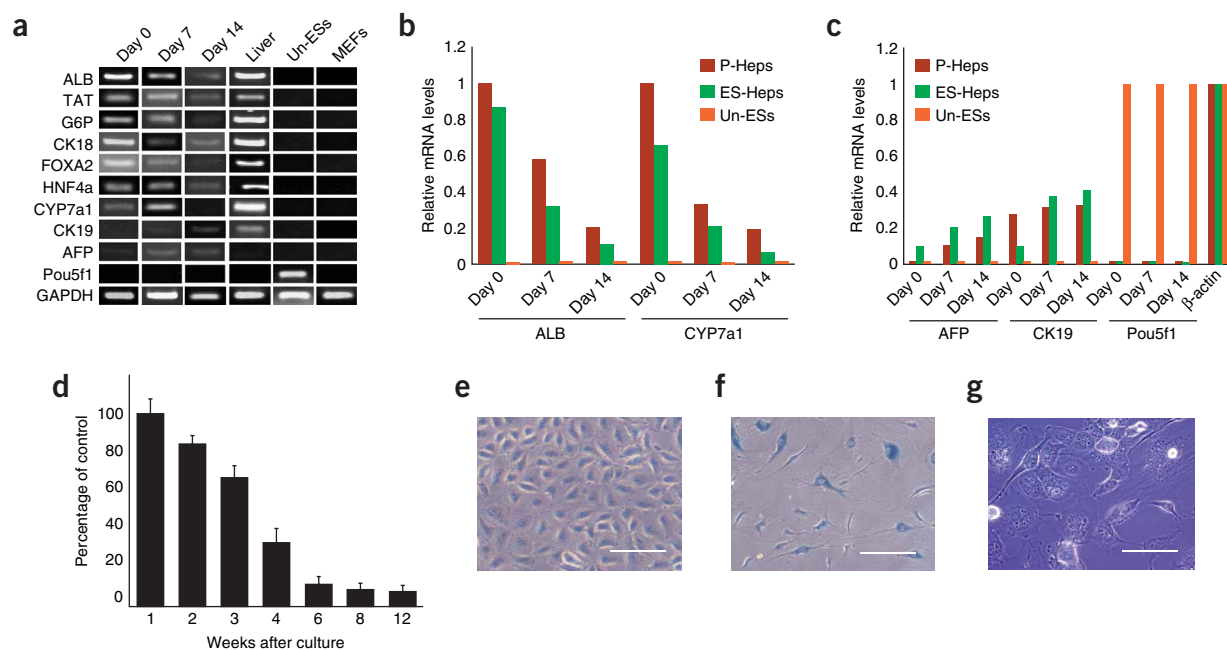


Figure 4 Fate of ES-Heps in long-term culture. ES-Heps were differentiated from mES cells and cultured under standard hepatocyte culture conditions for 12 weeks. **(a)** The expression of lineage-specific hepatic markers (ALB, TAT, G6P, CK18, CK19, and CYP7A1), endoderm markers (HNF-3 β , HNF-4 α , and AFP) and a marker for undifferentiated cells (Pou5f1) was analyzed by RT-PCR. **(b,c)** Expression profiles were confirmed by real-time PCR analysis, and mRNA expression levels were normalized relative to GAPDH. **(d)** ES-Heps (1×10^6) were inoculated into 6-well plates and the cell number of cultured ES-Heps was calculated weekly by trypan blue exclusion for 12 weeks. **(e–g)** ES-Heps were subjected to senescence-associated β -galactosidase staining after **(e)** 1 week and **(f)** 6 weeks of culture and **(g)** photographed under phase contrast after 6 weeks of culture. The data are representative of at least three independent experiments. AFP, alpha fetoprotein; ALB, albumin; CK18, cytokeratin-18; cytokeratin-19; CYP7A1, cytochrome P450; G6P, glucose-6-phosphate; HNF-3 β , hepatic nuclear factor-3 β ; HNF-4 α , hepatic nuclear factor-4 α ; TAT, tyrosine aminotransferase.

ES-Heps secreted albumin at 300–600 ng/ml/24 h/ 5×10^5 cells, $\sim 70\%$ of that produced by primary mouse hepatocytes, and metabolized $49 \pm 8.5\%$ of loaded ammonia, $32.3 \pm 2.8\%$ of lidocaine and $35.6 \pm 4.7\%$ of diazepam. ES-Heps derived without coculture with liver nonparenchymal cells (ES-non coculture-Heps) secreted albumin at 150–250 ng/ml/24 h/ 5×10^5 cells, $\sim 20\%$ of that produced by primary mouse hepatocytes, and metabolized only $21.3 \pm 3.0\%$ of loaded ammonia, $12.3 \pm 1.5\%$ of lidocaine and $14.6 \pm 3.0\%$ of diazepam. GFP-Ns and undifferentiated mouse ES cells produced no albumin and did not metabolize any of the above compounds (**Fig. 3j–m**).

We also examined the relative contribution of each cell line to the differentiation process. Coculture with liver endothelial (TMNK-1) cells was superior for generating albumin-promoter-derived GFP-positive cells and improved cell function better than coculture with the other two cell lines. Coculture of ES cells with all three cell lines maximized the differentiation process toward functional hepatocytes (**Supplementary Fig. 2** online).

Under light microscopy, ES-Heps were polygonal in shape, contained cytoplasmic granules (**Fig. 3n**) and uniformly expressed albumin (**Fig. 3o**). Transmission electron microscopy revealed glycogen granules (**Fig. 3p**), further suggesting that GFP-positive cells were hepatocytes. Hepatocyte-specific gene expression was enriched in MoFlo-sorted GFP-positive ES-Heps but expression diminished over time, as did the number of ES-Heps surviving in culture (**Fig. 4**). Expression of senescence-associated β -galactosidase by ES-Heps began to appear after 6 weeks in culture, indicating that ES-Heps, like primary mouse hepatocytes, become senescent in culture. We also determined whether ES-Heps produce undesirable

secreted proteins or proteins representing differentiation toward a nonhepatic phenotype. ES-Heps produced no proteases in culture and did not express gastrin, secretin or amylase (**Supplementary Fig. 3** online). Finally, transplantation of 1×10^6 ES-Heps into the subcutaneous tissue of severe combined immune deficiency (SCID) mice ($n=10$) generated no tumors over a 6-month observation period, whereas transplantation of 1×10^6 undifferentiated mouse ES-cells generated tumors 30–35 mm in diameter within 6 weeks of implantation.

Use of an ES-Hep-containing BAL in liver failure

To determine whether ES-Heps could correct a physiologically significant deficiency in hepatic function, we employed the 90% hepatectomy model of acute liver failure in mice, which produces hyperammonemia-induced hepatic encephalopathy, hypoglycemia and 100% mortality in animals within 4 d of hepatectomy. A liver assist device module consisting of a PAU-coated PTFE ethylene vinylalcohol copolymer (EVAL) membrane and a polyester supporting fabric coated by gelatinized FGF-2 (**Supplementary Figs. 4–6** online) was implanted into the subcutaneous tissue at the time of hepatectomy through a 10-mm abdominal incision. A cell injection port was then fixed in the subcutaneous space. We then introduced 5×10^6 primary mouse hepatocytes, undifferentiated ES cells, GFP-Ns, ES-non coculture-Heps or ES-Heps, equivalent to 5% of the mouse liver mass, into the device on the day of hepatectomy and 1 and 3 d after hepatectomy to produce a BAL.

Untreated mice that underwent 90% hepatectomy became hypoglycemic, their blood ammonia levels increased substantially and they developed encephalopathy. The response to hepatectomy was unaffected

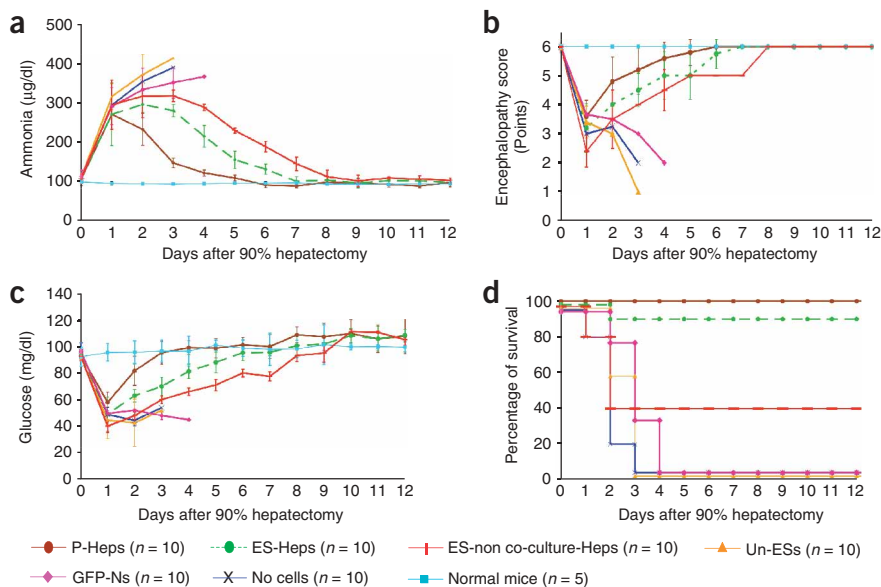


Figure 5 Ammonia, hepatic encephalopathy, blood glucose, and survival of hepatectomized mice after BAL therapy. Mice were hepatectomized (90% liver removal) and implanted with BAL modules containing primary hepatocytes (P-Heps), ES-Heps, ES-non coculture-Heps (derived under conditions where no coculture with liver non-parenchymal cells was performed), undifferentiated ES cells (Un-ESs), GFP-negative cells (GFP-Ns), or no cells. (a) Blood ammonia levels, (b) encephalopathy scores, (c) blood glucose levels, and (d) survival were determined for 12 d.

tomized mice treated with a BAL charged with undifferentiated ES cells or GFP-Ns died within 4 d of hepatectomy from acute liver failure, whereas 90% of hepatectomized mice treated with the BAL charged with ES-Heps survived (**Fig. 5d**) and had regenerated their remnant liver. Only 40% of hepatectomized mice treated with a BAL charged with ES-non coculture-Heps survived, indicating that

coculture significantly enhanced hepatocyte differentiation.

Characteristics of ES-Heps following use in the BAL

ES-Heps were examined 7 d after implantation of the BAL in hepatectomized mice with liver failure. Cells had attached to the surface of the PTFE membrane of the BAL module in a trabecular pattern (**Fig. 6a,b**) and transmission electron microscopy showed the

by treatment with a BAL charged with undifferentiated ES cells or GFP-Ns (**Fig. 5**). However, treatment with a BAL charged with ES-Heps caused blood glucose and ammonia levels to normalize by 6 d after induction of hepatic failure (**Fig. 5a,c**). Encephalopathy also reversed, most likely the result of correcting the blood ammonia level (**Fig. 5b**). These responses were identical to those seen after treatment with a BAL charged with primary mouse hepatocytes (**Fig. 5**). Finally, all hepatec-

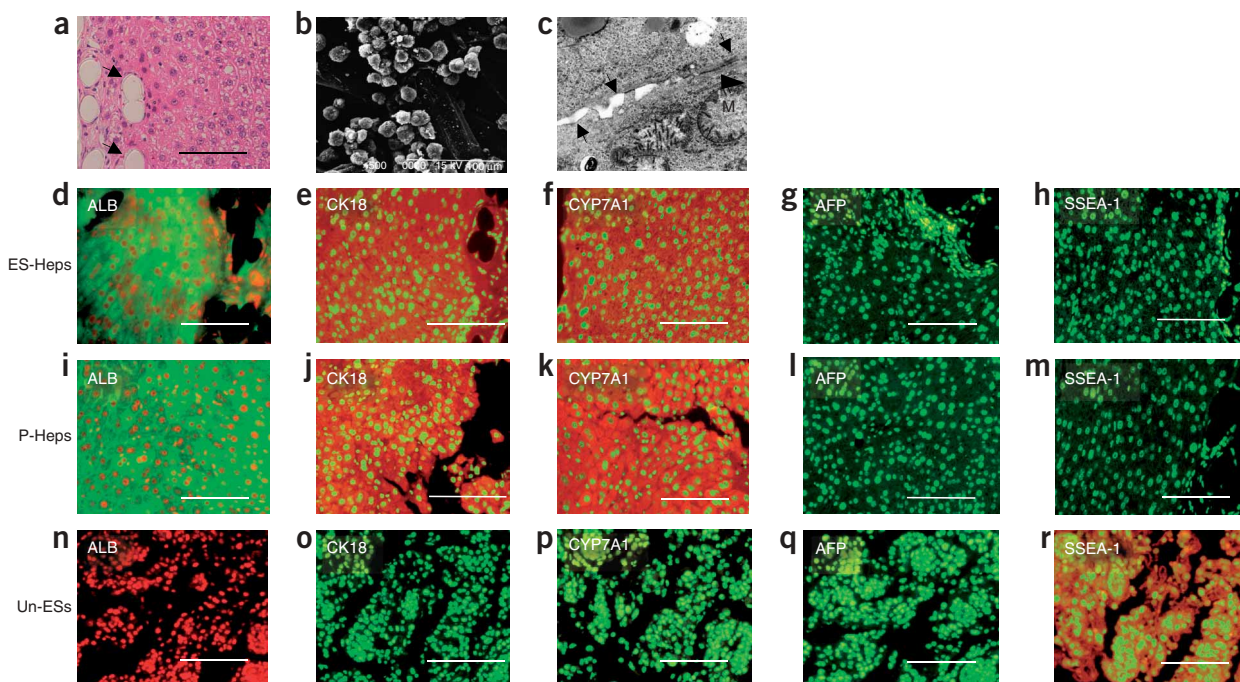


Figure 6 Morphologic and histological analysis of ES-Heps in BAL modules. Hepatectomized mice were implanted with BAL modules containing ES-Heps, primary hepatocytes (P-Heps), or undifferentiated ES cells (Un-ESs), and BAL modules were removed from surviving mice 7 d later. (a) HE staining showed the trabecular patterning of ES-Heps in BAL modules. Arrows indicate the PTFE cloth. (b) Scanning electron microscopy revealed attachment of ES-Heps on the surface of the PTFE cloth. (c) Transmission electron microscopy revealed the presence of bile canaliculi with apical microvilli; original magnification $\times 30,000$. (d–h) ES-Heps, (i–j) P-Heps, and (n–r) Un-ESs recovered from the BAL modules were immunostained for (d,i,n) albumin (green), (e,j,o) cytokeratin-18 (CK18; red), (f,k,p) cytochrome P450 (CYP7A1, red), (g,l,q) alpha-fetoprotein (AFP, red), or (h,m,r) stage-specific embryonic antigen-1 (SSEA-1, red). Nuclei were counter-stained with Dapi. Bars, 100 μm .

presence of glycogen rosettes, well-developed bile canaliculi with apical microvilli, and tight junctions (Fig. 6c). Immunohistochemistry of BAL-attached ES-Heps showed a pattern identical to that of primary mouse hepatocytes, staining positive for albumin, cytokeratin-18 and cytochrome P450, and negative for AFP and Pou5f1 (Fig. 6d–r).

DISCUSSION

In these studies, we present an improved and reproducible method for generating functional hepatocytes from pluripotent ES cells and a relatively simple design for artificial liver support using ES-Heps. If successful in patients, this approach would not require intensive hemodynamic monitoring. Although methods for hepatic differentiation of ES cells have been described, none have generated cells with function adequate for clinical use^{19–25} or with enough phenotypic uniformity to eliminate the risk of teratoma formation²⁶. We found that ES cell differentiation into cells with the capacity to function as hepatocytes was significantly enhanced by coculturing embryoid body cells with human liver nonparenchymal cells. Other investigators have demonstrated that exposure to damaged liver tissue stimulates liver cell regeneration and can enhance homing and differentiation of stem cells to a hepatocyte phenotype^{13,21}. Unfortunately, differentiation strategies using damaged liver tissues have limited clinical utility.

Our strategy involves culturing embryoid bodies with activin A and FGF-2 to enhance their differentiation to definitive endoderm as previously described^{27–29}. The critical importance of growth in activin A and FGF-2 to the differentiation process is demonstrated in **Supplementary Figs. 7 and 8** online. Next, recognizing the importance of heterotopic interactions between hepatocytes and hepatic nonparenchymal cells in liver development, we cocultured the endoderm-enriched cells with growth factors known to be important for hepatic differentiation^{30–33} *in trans*-well plates with MMC-C–treated conditionally immortalized human liver nonparenchymal cells to enhance differentiation toward functional hepatocytes. The human liver nonparenchymal cell lines were developed in our laboratory and provide an unlimited source of human cells for hepatic differentiation. The conditionally immortalized human cholangiocytes used for these studies (MMNK-1)¹⁶ generate interleukin-6 and TNF- α , the liver endothelial cells (TMNK-1)¹⁷ produce fibroblast growth factor (FGF)4 and vascular endothelial growth factor (VEGF), and the liver stellate cells (TWNT-1)¹⁸ produce HGF, all factors important for liver regeneration (**Supplementary Fig. 9** and **Supplementary Table 2** online). We incorporated dHGF, which lacks a 5–amino acid sequence in the first kringle domain of HGF³⁴, rather than the more commonly used HGF in our differentiation process because it is less cytotoxic than HGF when used at high doses in hepatocyte culture³⁴ (**Supplementary Fig. 10** online) and has twice the potency of HGF in stimulating DNA synthesis by rat hepatocytes³¹. The coculture differentiation strategy induced an $\sim 50\%$ increase in the number of ES cells becoming albumin positive, and resulted in 68.7% of the entire cell population differentiating toward a hepatocyte phenotype. The culture substrate also strongly affected the differentiation efficiency (**Supplementary Figs. 11 and 12** online).

The relevance of the procedure outlined here to human ES cells is unknown. However, differentiation of human ES cells using the PTFE cloth, rather than Matrigel, improves production of albumin and urea and metabolism of lidocaine³⁵, whereas high-dose dHGF, rather than HGF, further enhances differentiation (data not shown). Thus, the approach described here appears promising for application to human ES cells. However, cell sorting, as carried out here, may not be practical for isolating the billions of human ES cell–derived hepatocytes that would be needed to generate a clinically useful BAL, although

simultaneous use of several MoFlo machines could reduce the time required to a few hours. Alternatively, more rapid magnetic cell sorting, using asialoglycoprotein receptor (ASGPR)-mediated positive selection or undifferentiated marker-mediated negative selection could be used. If human ES cells could reliably be differentiated to functional human hepatocytes, efficient sorting techniques will need to be developed further.

To isolate ES-Heps, we used a plasmid vector expressing GFP from an albumin promoter. This approach generated high lineage-specific GFP expression by transient high copy number transfection and avoided the difficult step of producing ES cell lines that stably express exogenous genes. Creation of stable ES cell transfectants is especially difficult to accomplish with human ES cell lines that tolerate individual cell cloning poorly. The flow-sorted, albumin-positive cells functioned *in vitro* with two-thirds the capacity of primary mouse hepatocytes.

The design of the BAL eliminates the need for vascular connection to the patient, which produces circulatory instability and requires anticoagulation in patients with liver failure who are already at high risk for bleeding from low platelet counts and coagulation factor deficiencies. The BAL module consisted of an EVAL 30-nm pore size membrane that allows free exchange of glucose and ammonia and prevents the passage of lymphocytes from the host into the device and of the cells from the device into the host, further reducing the risk of teratoma formation. Attachment of the introduced cells was facilitated by the PAU-coated PTFE cloth, which also allowed the cells to engraft in a three-dimensional structure. The BAL was coated with FGF-2 to facilitate rapid vascularization around the module surface³⁶ where engrafted cells remained viable for up to 16 weeks (data not shown), longer than previously reported^{37,38}. Finally, the cell injection port allows repeated inoculation of the BAL with fresh cells to facilitate maintenance of a functional hepatocyte mass. Use of this device in mice with acute liver failure, which uniformly die within 4 d of inducing hepatic failure, resulted in 90% animal survival.

In summary, these mouse studies provide a foundation for differentiation of functional hepatocytes from human ES cells and a practical design for a clinically useful liver-assist device. Further studies will be needed to determine whether these methods can be adapted for use in patients.

METHODS

Animal experiments. Female Balb/c SCID mice (Nippon CLEA) were used for all transplantation procedures. Balb/c mice (Nippon CLEA) were used for hepatocyte isolation. All procedures performed on the animals were approved by the Okayama University Institutional Animal Care and Use Committee, and thus within the guidelines for humane care of laboratory animals.

Differentiation and purification of mES cells in culture. Mouse ES cells derived from Balb/c \times 129sv embryos were expanded on a feeder layer of mitomycin-treated mouse embryonic fibroblasts¹, seeded on 0.1% gelatin-coated plates (R-ES-006B, Dainippon Pharmaceutical Co.), and cultured in Dulbecco's Modified Eagle Medium containing 15% FBS, 1% nonessential amino acid, 1% nucleosides, 2-mercaptomethanol (110 μ M), 1% penicillin/streptomycin, 1% glutamic acid, and 500 U/ml leukemia inhibitory factor (Dainippon Pharmaceutical Co.). ES cells (2.5×10^5 cells/ml) were suspended, inoculated into ultra-low attachment chamber (Corning), and cultured for 2 d without leukemia inhibitory factor. The resulting embryoid bodies were transferred onto an unwoven PTFE cloth coated with PAU, which has cellular adhesive properties (Kuraray Medical Co.), and treated for 3 d with 100 ng/ml FGF-2 (PreproTech EC) and 100 ng/ml activin A (R & D Systems Co.) using Dulbecco's Eagle medium Nutrient Mixture F-12 (Gibco BRL), containing 1% FBS (Gibco BRL), 4.5 mg/ml glucose, 2 μ M L-glutamine, 25 μ M HEPES (Gibco BRL), 3% albumin from bovine serum (Sigma), 100 U/ml penicillin,

and 100 µg/ml streptomycin (Sigma) (Fig. 1). The cells were then continuously cultured on the PAU-coated PTFE fabric, while the upper chamber, isolated by a 0.4 µm pore size trans-well membrane (Becton Dickinson) was seeded with 5×10^5 mitomycin C-treated (MMC; Sigma, 10 mg/ml for 2 h) conditionally immortalized human cholangiocyte cells (MMNK-1 cells¹⁶), 5×10^5 liver endothelial cells (TMNK-1 cells¹⁷) and 5×10^5 hepatic stellate cells (TWNT-1 cells¹⁸) in Dulbecco's Eagle medium Nutrient Mixture F-12 (Gibco BRL), containing 4.5 mg/ml glucose, 2 µM L-glutamine, 25 µM HEPES (Gibco BRL) 100 U/ml penicillin, and 100 µg/ml streptomycin (Sigma) for 8 d with 100 ng/ml dHGF, 1% dimethyl sulfoxide and 10% FBS. For the final 3 d of culture, cells were treated with 10^{-7} M dexamethasone (Sigma). The cells were trypsinized, suspended as single cells, and transfected using Nucleofector (Amaxa Biosystems), according to the manufacturer's specifications, with a plasmid vector containing green fluorescent protein cDNA under the control of the albumin promoter (pALB-GFP). GFP expression was determined using a MoFlo cell sorter (DakoCytomation Co.), the data were analyzed by Software Summit v3.1 (DakoCytomation Co.), and GFP-positive cells, referred to as ES-Heps, were recovered for further study by MoFlo. Cells that failed to express GFP, referred to as GFP-Ns, were similarly recovered and used as negative controls for some experiments.

Mouse hepatocyte isolation and culture. For use as a positive control, primary hepatocytes were isolated from Balb/c mice weighing 20 g (Nippon CLEA) using a two-step collagenase digestion method, as previously reported³⁹. The yield and viability of the isolated hepatocytes were $1.0\text{--}1.5 \times 10^7$ cells per animal and >90%, respectively.

Evaluation of metabolic capacity and albumin secretion by ES-Heps. We seeded 5×10^5 primary mouse hepatocytes, undifferentiated ES cells, ES cell-derived GFP-Ns, ES-non coculture-Heps or ES-Heps into the wells of a 12-well tissue culture plate. Individual wells were coated with a PAU-treated PTFE cloth, which provided a stable three-dimensional cell matrix for cell growth⁴⁰. Ammonium sulfate (0.56 mM), lidocaine (1 mg/ml) and diazepam (1 µg/ml) were added to individual wells 24 h later, and the amount of each substrate remaining in the medium after culture for 24 h was measured. The ammonia concentration was determined using a Fuji Dri-Chem slide (Fuji) and concentrations of lidocaine and diazepam were measured by SRL. We measured 24-h albumin secretion into the culture medium using a mouse albumin enzyme-linked immunosorbent assay (ELISA) kit and metabolic rate was calculated as previously described³⁴.

Gene expression analyses. Total RNA was extracted from 1×10^6 ES-Heps, GFP-Ns cells, undifferentiated mouse ES cells, mouse liver and mouse embryonic fibroblasts (1×10^6 cells) during various stages of the differentiation process, and following MoFlo isolation and culture of ES-Heps and GFP-Ns, using RNA Trizol (Invitrogen) according to the manufacturer's protocol.

RT-PCR was performed at 22°C for 10 min and then at 42°C for 20 min using 1.0 µg of RNA per reaction, to ensure that the amount of cDNA amplified was proportional to the mRNA present in the original samples as previously reported⁴¹ using specific primers. The following specific primers were used: albumin (AJ011413): sense strand: 5'-GACAAGGAAAGCTGCCTGAC-3', antisense strand: 5'-TTCTGCAAAGTCAGCATTGG-3'; TAT (BC025934): sense strand: 5'-ACCTTCAATCCCATCCGA-3', antisense strand: 5'-TCCCGACTGGA TAGGTAG-3'; G6P (U00445): sense strand: 5'-CAGGACTGGTTCATCCTT-3', antisense strand: 5'-GTTGCTGTAGTAGTCGGT-3'; CK 18 (XM356490): sense strand: 5'-CGATACAAGGCACAGATGGA-3', antisense strand: 5'-CTTCTCCATCCTCCAGCAAG-3'; HNF3 β (U04197): sense strand: 5'-TATTGGCTGCAGCTAAGCGG-3', antisense strand: 5'-GACTCGGACTCAGGTGA GGT-3'; HNF4 α (NM8261) sense strand: 5'-ATTCTCCAACAGCCTGAGC-3', antisense strand: 5'-CGTCTGTGATGTTGGCAATC-3'; CYP 7A1 (AK050260) sense strand: 5'-AGGACTTCACTTACACC-3', antisense strand: 5'-GCAGTCGTTACATCATCC-3'; CK 19 (M36120) sense strand: 5'-GTGCCACCATTGACAATCC-3', antisense strand: 5'-AATCCACCTCCACACTGACC-3'; AFP (V00743) sense strand: 5'-CACTGCTGCAACTCTTCGTA-3', antisense strand: 5'-CTTTGGACCCTCTTCTGTGA-3'; Pou5f1 (NM013633) sense strand: 5'-GGCGTTCCTTTGGAAAGGTGTTCC-3', antisense strand: 5'-CTCGAACCCATCCTTCTCT-3', and glyceraldehyde-3-phosphate dehydrogenase (GAPDH)

(NM001001303): sense strand: 5'-TGAAGGTCGGTGTGAACGGATTTGGC-3', antisense strand: 5'-TGTTGGGGGCCGAGTTGGGATA-3'. After hybridization with labeled probes, the hybridized bands were detected by radiography.

The PCR products were resolved on 1% agarose gels and visualized by ethidium bromide staining. Mouse glyceraldehyde-3-phosphate dehydrogenase (GAPDH) served as an internal control for the efficiency of mRNA isolation and cDNA synthesis. Real-time RT-PCR was performed as previously described using the LightCycler instrument and aLightCycler FastStart DNA Master SYBR Green I kit (Roche Diagnostics)⁴¹. Briefly, 0.1 µg of total RNA from each sample was prepared for reverse transcription, and PCR was performed in a 20 µl reaction volume in triplicate using specific primers for each gene. mRNA copy numbers were calculated from serially diluted standard curves generated from a cDNA template, which represented *in vitro* samples, and bands were confirmed with gel electrophoresis. Data was analyzed using LightCycler Software (Roche Molecular Biochemicals). All expression levels were normalized to the beta-actin control. The relative expression of genes normally expressed in the liver was determined based on the mRNA level relative to that obtained from the normal adult mouse liver. The relative expression of other genes was determined based on the mRNA level relative to the beta-actin control. After hybridization with labeled probes, the hybridized bands were detected by radiography.

Electron microscopic examination. GFP-positive ES-Heps were fixed with 4% paraformaldehyde and 0.1% glutaraldehyde in 0.1 M phosphate buffer, pH 7.4 both immediately after MoFlo sorting and after 7 d of growth in the subcutaneously implanted BAL module. Electron microscopy was performed as previously described⁴¹. Ten different areas were randomly chosen for examination.

Measurement of cell viability and senescence. One million ES-Heps were inoculated into each well of a 24-well plate (BD Biosciences) and their growth and viability was measured by MTT assay using 0.5 mg/ml of 3-(4,5-dimethylthiazole-2-yl)-2,5-diphenyl tetrazolium bromide (MTT reagent) (Sigma), as previously described³⁴. After treatment with 0.5%EDTA-trypsin (Sigma), the number of viable hepatocytes was counted using a trypan blue exclusion test and compensated for the analysis. Senescence-associated β-galactosidase staining was also performed. Briefly, ES-Heps were washed in PBS, fixed in 0.25% glutaraldehyde for 10 min on ice, and incubated at 37 °C with a fresh staining solution consisting of 1 mg/ml of 5-bromo-4-chloro-3-indolyl β-D-galactoside, 40 mM citric acid-sodium phosphate (pH 6.0), 5 mM potassium ferricyanide, 5 mM potassium ferrocyanide, 150 mM NaCl, and 2 mM MgCl₂. Staining was performed as previously described⁴².

Construction of the BAL module. The BAL module was constructed using a polyethylene-vinyl alcohol membrane (30 nm pore size), which inhibits passage of immune competent cells and C3 and thus provides a degree of immune isolation, and a PAU-coated PTFE non-woven fabric, which provides a substrate for cell adhesion. The 15 × 15 mm PTFE fabric was covered with an EVAL membrane and layered with a piece of polyester supporting fabric of equal size to generate an inside BAL volume of 1.125 ml. A cell injection port was then attached. To facilitate angiogenesis around the implanted module, both surface layers of the BAL module were coated with gelatinized FGF-2 before implantation³⁶.

Induction of acute liver failure in mice and BAL implantation. Eight week-old female Balb.SCID mice (Nippon CLEA) underwent 90% hepatectomy to induce hepatic failure¹¹. Both sides of a BAL module were coated by 2 mg of gelatinized FGF-2 microspheres³⁶. Directly after hepatectomy, a BAL module was implanted subcutaneously on to the abdominal wall. Twelve, 36, and 60 h after implantation, 5×10^6 mouse primary hepatocytes, ES-Heps, GFP-Ns cells, or undifferentiated mouse ES cells were introduced in 200 µl Matrigel (BD Biosciences) and 0.5 ml culture medium into the BAL module through a subcutaneously fixed cell injection port, which was designed for easy exterior access to facilitate multiple cell infusions. To prevent animal dehydration, 1 ml of saline was injected intra-abdominally into each mouse for the first 3 d after hepatectomy. Blood was collected for levels of ammonia and glucose as previously described^{34,39}. Hepatic encephalopathy was measured by means of a 6 point coma scale consisting of measurements of flexion, grasping, righting,

placement, corneal and head-shaking reflexes (6 points indicating normal behavior)³⁹. Vascularization around the BAL implantation site was evaluated using a laser doppler tissue blood flow imager (Advance) and quantification was determined using Laser FlowGraphy (LFG-1 version 1.0, Softcare)⁴³.

Histological analyses. Differentiating mouse ES cells were embedded in medium for frozen tissue (Tissue-Tek) on days 7 and 14 of differentiation. Samples were then incubated with a polyclonal rabbit anti-mouse albumin (Cedarlane) and a polyclonal rabbit anti-mouse AFP (Santa Cruz Biotech) for analysis, as outlined below. Autopsies were also performed at the time of death or sacrifice. BAL samples were fixed with 20% formalin, embedded in paraffin, and processed for staining with hematoxylin and eosin. Additional BAL samples were incubated with polyclonal rabbit anti-mouse albumin or polyclonal rabbit anti-mouse cytokeratin-18, polyclonal rabbit anti-mouse cytochrome P450, polyclonal rabbit anti-mouse AFP, or mouse monoclonal anti-stage-specific embryonic antigen-1 (SSEA-1) (Santa Cruz Biotech), followed by Cy2- or Cy3-labeled secondary antibody (Amersham Biosciences). Samples were observed under a confocal laser scanning microscope (LSM510; Carl Zeiss).

Statistical analyses. Mean values are presented with standard deviations. ANOVA was used to calculate the significance of difference in mean values. The Kaplan-Meier method was used to calculate survival, and significance was determined by the Mann-Whitney *U* test. A *P* value <0.05 was considered statistically significant.

Note: Supplementary information is available on the Nature Biotechnology website.

ACKNOWLEDGMENTS

This research was supported in part by a Grant-in-Aid for Scientific Research (B) of the Japan Society for the Promotion of Science to N.K. and National Institutes of Health grant DK48794 to I.J.F. We thank Donna B. Stolz for useful comments for the paper. We thank Ann Kyle for editorial assistance.

AUTHOR CONTRIBUTIONS

Ira J. Fox and Naoya Kobayashi had full access to all of the data in the study and take responsibility for the integrity of the data and the accuracy of the data analyses. Study concept and design, I.J.F., N.K., A.S.-G., J.L., J.-W.Y., H.-S.J., N.T. Acquisition of data, I.J.F., N.K., A.S.-G., N.T. Analysis and interpretation of data, I.J.F., N.K., A.S.-G. Drafting of the manuscript, I.J.F., N.K., A.S.-G., J.L., J.-W.Y., H.-S.J. Critical revision of the manuscript for important intellectual content, I.J.F., N.K., A.S.-G. Statistical analysis, T.O., H.N. Obtained funding, I.J.F., N.K. Administrative, technical, or material support, I.J.F., N.K., A.S.-G., N.N.-A., J.D.R.-C., H.B., T.U., Y.T., D.Z., Y.C., K.T., M.N., A.M. Study supervision, I.J.F., N.K. All authors contributed to the preparation of the report.

COMPETING INTERESTS STATEMENT

The authors declare competing financial interests (see the *Nature Biotechnology* website for details).

Published online at <http://www.nature.com/naturebiotechnology/>

Reprints and permissions information is available online at <http://npg.nature.com/reprintsandpermissions/>

- Lee, W.M. Acute liver failure. *N. Engl. J. Med.* **329**, 1862–1872 (1993).
- Williams, R. & Wendon, J. Indications for orthotopic liver transplantation in fulminant liver failure. *Hepatology* **20**, S5–S10 (1994).
- Abe, T. *et al.* Study of plasma exchange for liver failure: beneficial and harmful effects. *Ther. Apher. Dial.* **8**, 180–184 (2004).
- Rifai, K. *et al.* Prometheus—a new extracorporeal system for the treatment of liver failure. *J. Hepatol.* **39**, 984–990 (2003).
- Sen, S. *et al.* Pathophysiological effects of albumin dialysis in acute-on-chronic liver failure: a randomized controlled study. *Liver Transpl.* **10**, 1109–1119 (2004).
- Chen, S.C. *et al.* Treatment of severe liver failure with a bioartificial liver. *Ann. NY Acad. Sci.* **831**, 350–360 (1997).
- Demetriou, A.A. *et al.* Prospective, randomized, multicenter, controlled trial of a bioartificial liver in treating acute liver failure. *Ann. Surg.* **239**, 660–667, discussion 667–670 (2004).
- Nagata, H. *et al.* Treatment of cirrhosis and liver failure in rats by hepatocyte xenotransplantation. *Gastroenterology* **124**, 422–431 (2003).
- Platt, J.L. Xenotransplanting hepatocytes: the triumph of a cup half full. *Nat. Med.* **3**, 26–27 (1997).

- van de Kerkhove, M.P. *et al.* Evidence for Gal α (1–3)Gal expression on primary porcine hepatocytes: implications for bioartificial liver systems. *J. Hepatol.* **42**, 541–547 (2005).
- Kobayashi, N. *et al.* Prevention of acute liver failure in rats with reversibly immortalized human hepatocytes. *Science* **287**, 1258–1262 (2000).
- Alison, M.R. *et al.* Hepatocytes from non-hepatic adult stem cells. *Nature* **406**, 257 (2000).
- Jang, Y.Y., Collector, M.I., Baylin, S.B., Diehl, A.M. & Sharkis, S.J. Hematopoietic stem cells convert into liver cells within days without fusion. *Nat. Cell Biol.* **6**, 532–539 (2004).
- Lagasse, E. *et al.* Purified hematopoietic stem cells can differentiate into hepatocytes in vivo. *Nat. Med.* **6**, 1229–1234 (2000).
- Schwartz, R.E. *et al.* Multipotent adult progenitor cells from bone marrow differentiate into functional hepatocyte-like cells. *J. Clin. Invest.* **109**, 1291–1302 (2002).
- Maruyama, M. *et al.* Establishment of a highly differentiated immortalized human cholangiocyte cell line with SV40T and hTERT. *Transplantation* **77**, 446–451 (2004).
- Matsumura, T. *et al.* Establishment of an immortalized human-liver endothelial cell line with SV40T and hTERT. *Transplantation* **77**, 1357–1365 (2004).
- Watanabe, T. *et al.* Establishment of immortalized human hepatic stellate scavenger cells to develop bioartificial livers. *Transplantation* **75**, 1873–1880 (2003).
- Yamamoto, H. *et al.* Differentiation of embryonic stem cells into hepatocytes: biological functions and therapeutic application. *Hepatology* **37**, 983–993 (2003).
- Rambhatla, L., Chiu, C.P., Kundu, P., Peng, Y. & Carpenter, M.K. Generation of hepatocyte-like cells from human embryonic stem cells. *Cell Transplant.* **12**, 1–11 (2003).
- Lavon, N., Yanuka, O. & Benvenisty, N. Differentiation and isolation of hepatic-like cells from human embryonic stem cells. *Differentiation* **72**, 230–238 (2004).
- Yamada, T. *et al.* In vitro differentiation of embryonic stem cells into hepatocyte-like cells identified by cellular uptake of indocyanine green. *Stem Cells* **20**, 146–154 (2002).
- Teratani, T. *et al.* Direct hepatic fate specification from mouse embryonic stem cells. *Hepatology* **41**, 836–846 (2005).
- Teramoto, K. *et al.* Teratoma formation and hepatocyte differentiation in mouse liver transplanted with mouse embryonic stem cell-derived embryoid bodies. *Transplant. Proc.* **37**, 285–286 (2005).
- Chinzei, R. *et al.* Embryoid-body cells derived from a mouse embryonic stem cell line show differentiation into functional hepatocytes. *Hepatology* **36**, 22–29 (2002).
- Fujikawa, T. *et al.* Teratoma formation leads to failure of treatment for type 1 diabetes using embryonic stem cell-derived insulin-producing cells. *Am. J. Pathol.* **166**, 1781–1791 (2005).
- D'Amour, K.A. *et al.* Efficient differentiation of human embryonic stem cells to definitive endoderm. *Nat. Biotechnol.* **23**, 1534–1541 (2005).
- Yasunaga, M. *et al.* Induction and monitoring of definitive and visceral endoderm differentiation of mouse ES cells. *Nat. Biotechnol.* **23**, 1542–1550 (2005).
- Kubo, A. *et al.* Development of definitive endoderm from embryonic stem cells in culture. *Development* **131**, 1651–1662 (2004).
- Block, G.D. *et al.* Population expansion, clonal growth, and specific differentiation patterns in primary cultures of hepatocytes induced by HGF/SF, EGF and TGF alpha in a chemically defined (HGM) medium. *J. Cell Biol.* **132**, 1133–1149 (1996).
- Oh, S.H. *et al.* Hepatocyte growth factor induces differentiation of adult rat bone marrow cells into a hepatocyte lineage in vitro. *Biochem. Biophys. Res. Commun.* **279**, 500–504 (2000).
- Jung, J., Zheng, M., Goldfarb, M. & Zaret, K.S. Initiation of mammalian liver development from endoderm by fibroblast growth factors. *Science* **284**, 1998–2003 (1999).
- Serra, R. & Isom, H.C. Stimulation of DNA synthesis and protooncogene expression in primary rat hepatocytes in long-term DMSO culture. *J. Cell. Physiol.* **154**, 543–553 (1993).
- Chen, Y. *et al.* Transplantation of human hepatocytes cultured with deleted variant of hepatocyte growth factor prolongs the survival of mice with acute liver failure. *Transplantation* **79**, 1378–1385 (2005).
- Soto-Gutierrez, A. *et al.* Differentiation of Human Embryonic Stem Cells to Hepatocytes Using Deleted Variant of HGF and Poly-amino-urethane-coated Non-woven Polytetrafluoroethylene Fabric. *Cell Transplant.* **15**, 335–342 (2006).
- Wang, W. *et al.* Reversal of diabetes in mice by xenotransplantation of a bioartificial pancreas in a prevascularized subcutaneous site. *Transplantation* **73**, 122–129 (2002).
- Gomez, N. *et al.* Evidence for survival and metabolic activity of encapsulated xenogeneic hepatocytes transplanted without immunosuppression in Gunn rats. *Transplantation* **63**, 1718–1723 (1997).
- Roger, V. *et al.* Internal bioartificial liver with xenogeneic hepatocytes prevents death from acute liver failure: an experimental study. *Ann. Surg.* **228**, 1–7 (1998).
- Kobayashi, N. *et al.* Hepatocyte transplantation in rats with decompensated cirrhosis. *Hepatology* **31**, 851–857 (2000).
- Ikeda, H. *et al.* Perfect control of blood glucose in totally pancreatectomized diabetic pigs using a newly developed bioartificial pancreas. *Tissue Eng.* (in the press) (2006).
- Narushima, M. *et al.* A human beta-cell line for transplantation therapy to control type 1 diabetes. *Nat. Biotechnol.* **23**, 1274–1282 (2005).
- Noguchi, H. *et al.* Controlled expansion of human endothelial cell populations by Cre-loxP-based reversible immortalization. *Hum. Gene Ther.* **13**, 321–334 (2002).
- Rafael, E., Gazelius, B., Wu, G.S. & Tibell, A. Longitudinal studies on the microcirculation around the TheraCyte immunoisolation device, using the laser Doppler technique. *Cell Transplant.* **9**, 107–113 (2000).

Erratum: Rainbow biotech—South Africa's emerging sector

Sabine Louët

Nat. Biotechnol. 24, 1313–1316 (2006); published online 2 November 2006.

In the version of the article initially published, on page 1316, paragraph 4, line 17, the interest rate of the eGoliBio incubator is erroneous. Instead of 3%, the rate is actually prime rate less 3%, which is ~10%. The text should read “They also have access to Rand 100,000 (\$12,600) loans at prime less 3% interest-rate....”

Corrigendum: Reversal of mouse hepatic failure using an implanted liver-assist device containing ES cell-derived hepatocytes

Alejandro Soto-Gutiérrez, Naoya Kobayashi, Jorge David Rivas-Carrillo, Nalu Navarro-Álvarez, Debaio Zhao, Teru Okitsu, Hirofumi Noguchi, Hesham Basma, Yashuhiko Tabata, Yong Chen, Kimiaki Tanaka, Michiki Narushima, Atsushi Miki, Tadayoshi Ueda, Hee-Sook Jun, Ji-Won Yoon, Jane Lebkowski, Noriaki Tanaka & Ira J Fox

Nat. Biotechnol. 24, 1412–1419 (2006); published online 5 November 2006; corrected after print 7 February 2007.

In the version of the article initially published, the fifth author's name is misspelled. The correct spelling is Debiao Zhao. The error has been corrected in the HTML and PDF versions of the article.

Corrigendum: Expression of artificial microRNAs in transgenic *Arabidopsis thaliana* confers virus resistance

Qi-Wen Niu, Shih-Shun Lin, Jose Luis Reyes, Kuan-Chun Chen, Hui-Wen Wu, Shyi-Dong Yeh & Nam-Hai Chua

Nat. Biotechnol. 24, 1420–1428 (2006); published online 22 October 2006; corrected after print 7 February 2007.

In the version of the article initially published, in the Author Contributions, the initials of the last author responsible for the virus challenge and related experiments are H.-W.W. and not H.-W.N., as originally indicated. In Figure 2e, the amiR-P69¹⁵⁹ line is line number 1 and not line number 11, as originally indicated. The error has been corrected in the PDF version of the article.